Radboud Universiteit

Bachelor thesis Physics and Astronomy

Institute for Mathematics, Astrophysics and Particle Physics (IMAPP)

Searching for Extragalactic Fast X-ray Transients in the Chandra Data Archive

J.L. Crans
Author

prof. dr. P.G. Jonker
Supervisor

prof. dr. P.G. Jonker
First Assessor

prof. A.J. Levan
Second Assessor

August 4, 2025

Fast X-ray Transients (FXTs) are short bursts of x-ray radiation typically lasting from a few minutes to multiple hours. There are many different scenarios for the origin of FXTs, one of which is off-axis gamma ray burst (GRB) afterglow. However, the FXTs this theory predicts, are longer in duration than currently found FXTs. We use a search algorithm to find FXT candidates in the Chandra Data Archive. Our main goals are: to find FXT candidates in not yet analysed data and to find longer FXT candidates, predicted by the off-axis GRB afterglow model.
In total we identify 50 candidates, of which: 20 are previously found FXTs, two are candidates from new data and five are candidates for longer duration FXTs. All candidates still need to be manually confirmed or ruled out as FXTs. If even a small fraction of candidates is confirmed as FXTs, it would significantly impact the event rate and, consequently, the potential origins of FXTs. Additionally, whether the long-duration candidates are confirmed as FXTs will also have an effect on the idea that FXTs are related to off-axis gamma-ray burst afterglows.

Contents

Chapter 1

Introduction

Fast X-ray Transients (FXTs) are short bursts of x-ray radiation lasting from a few minutes to multiple hours. These flashes are of unknown origin and are detected only once, making them inherently mysterious and very intriguing to explore. Figure 1.1 shows a light curve of an FXT, to serve as an example.

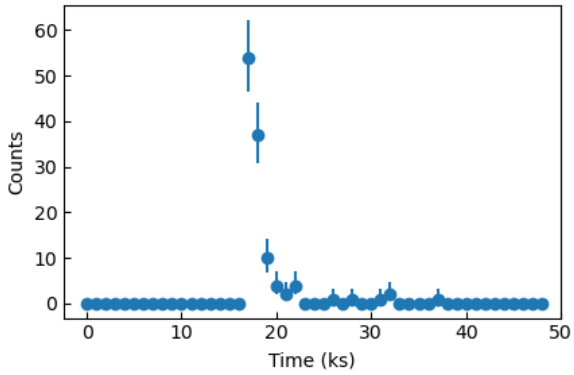

Figure 1.1 The light curve of the XT1 FXT found by Bauer et al. (2017), to serve as an example of what an FXT looks like. The light curve is a relation of counts per time interval.

Previous FXTs have mainly been identified in archival data, serendipitously and more recently through systematic searches (Quirola-Vásquez et al., 2022; Quirola-Vásquez et al., 2023). Because the FXTs are searched for in archival data, they are mostly identified long after the event initially took place. This makes it difficult to find multi-wavelength counterparts[1] of the FXT event, which in turn makes it more challenging to determine the origin of an FXT.

There are several possible origins of FXTs. Including super nova shock breakout, which releases x-rays when the shockwave of a core-collaps supernova reaches the surface of the star (Waxman and Katz, 2017); and tidal disruption events, that occur between stars and black holes. Specifically, a white dwarf and an intermediate mass black hole in the cases of FXTs, XRT 000519 and XRT 110103 (Jonker et al., 2013; Glennie et al., 2015). Another theory proposed by Wichern et al. (2024) suggests FXTs could be caused by off-axis gamma ray burst (GRB) afterglow, which is caused by the high energy particles, emitted from the GRB encountering interstellar media. However, the predicted FXTs are much longer in duration than the current sample of FXTs.

In total twenty-two extragalactic FXTs were identified by Quirola-Vásquez et al., 2022; Quirola-Vásquez et al., 2023, from here on mentioned as papers I and II. These papers adopt a method of finding FXTs developed by

[1] Multi-wavelength counterparts refer to detections of the same event, but in another part of the spectrum.

Yang et al. (2019). We will build on the work of papers I and II by conducting multiple searches, using the same search method, with the goal of finding new FXT candidates. Both of similar length to the current sample of FXTs, but also of longer duration as modelled in the work of Wichern et al. (2024). Like papers I and II, we will use the archival data of the Chandra x-ray satellite. This data was publicly released from 2000-02-03 to 2024-05-20 and can be accessed through the `CIAO` Chandra data analysis tool (Fruscione et al., 2006), provided by the Chandra X-ray Center (CXC).

In this thesis we will discuss: the search algorithm and filtering criteria (Sect. 2), the results of the searches (Sect. 3) and conclusions and further research possibilities (Sect. 4).

Chapter 2

Methodology

In this chapter we discuss: terminology used in the rest of this work (Sect. 2.1), the search algorithm for detecting FXT candidates (Sect. 2.2), what Chandra data is searched (Sect. 2.3), the extraction of sources from Chandra data (Sect. 2.4) and the filtering criteria to discard non FXT detections (Sect. 2.5).

2.1 Terminology

To make the rest of this chapter easier to follow, we will lay out the terminology used in the rest of this work, in this section.

First, terms we will use to describe the various stages in the process of Chandra observation to FXT candidate. We will refer to raw Chandra data as **observations**, observations having been analysed by the search algorithm as **analysed** observations, sources extracted from these observations as **sources**, sources marked as possible FXTs by the search algorithm as **detections** and detections that have passed every filter as **candidates**.

This work largely builds on the methods developed in papers I and II. We thus divide the observations into parts coinciding with the observation periods of these papers. The paper I period refers to the start of the Chandra mission up to 2015-01-01. The paper II period refers to the period from 2015-01-01 up to 2022-04-01. The new data period refers to the period from 2022-04-01 until 2024-05-20.

2.2 Search Algorithm

We adopt the same search algorithm as papers I and II with the goal of finding FXT candidates in the Chandra archive data. Possible FXTs are identified by searching for (parts of) light curves that have a high variance in their number of photon counts.

The algorithm analyses the light curve of a source in the following way. We first obtain the total number of counts of a source, N_{tot}, and the number of counts resulting from background radiation, N_{bkg}. Secondly, we divide the light curve into four quartiles, which we combine again into multiple regions that will be compared in their number counts.

Let's say the light curve starts at 0 and ends at t. This gives the quartiles: $q_1 = \left[0, \frac{t}{4}\right)$, $q_2 = \left[\frac{t}{4}, \frac{t}{2}\right)$, $q_3 = \left[\frac{t}{2}, \frac{3t}{4}\right)$, $q_4 = \left[\frac{3t}{4}, t\right]$. From these quartiles we can get the numbers of counts in the first half, second half, outer half and inner half, given by $N_1 = q_1 + q_2$, $N_2 = q_3 + q_4$, $N_1' = q_1 + q_4$ and $N_2' = q_2 + q_3$, respectively.

A source is marked as a detection when the following conditions are satisfied.

(i) $N_{\text{tot}} > 5 \times N_{\text{bkg}}$

(i) N_1 and N_2 are statistically different at a $> 5\sigma$ confidence level.

(i) Either, $N_1 > 5 \times N_2$ or $N_2 > 5 \times N_1$

The same conditions are checked for N_1' and N_2'.

To mitigate the effect of background radiation we apply this same procedure on segments of the light curve called windows. This is done in three passes to cover cases where transients fall on borders of the two comparing regions. In these cases, the counts across N_1 and N_2 might be similar, because the transient spans both halves.

As an example, lets say our light curve starts at 0 and ends at $T_{\text{exp}} = 48$ ks and take $T_{\text{window}} = 20$ ks, since that is the window size papers I and II used in their search and that we will use for a part of our search as well.

- **Forward pass.** We start at 0 and incrementally make windows of the chosen size up to the largest multiple that fits inside T_{exp}. The remaining time is also added and we call this the residual window. In this case we get $(0, 20), (20, 40), (40, 48)$.
- **Backward pass.** We now start at T_{exp} and replicate the forward pass in reverse. In this case we get $(48, 28), (28, 8), (8, 0)$.
- **Shifted pass.** We start this by first adding a window from 0 to half the size of the window, continuing from there. In this case we get $(0, 10), (10, 30), (30, 48)$.

2.2.1 Detection Probability Simulation

To demonstrate the effectiveness of this algorithm in detecting FXTs we replicate the simulation from paper I. We use the light curve shape of FXT, XT1 and randomly generate new light curves from the same temporal and spectral distributions. We also randomize the starting time of the transient within the observation to emulate a real data set. We then run the search algorithm on these randomly generated observations to get a detection probability for a variety of parameters. In figure 2.1 we display the detection probability of various window sizes.

A simulation of the detection probability for the longer FXTs we expect to find is a more difficult problem. Since we have not yet found an FXT with the expected longer duration, we do not have a sample to simulate the algorithm on. Additionally the FXT light curves simulated in the work of Wichern et al. (2024) have wildly varying shapes, which further indicates, that a single sample simulation would not give an accurate estimate for the detection probability.

2.2.2 Changes to the algorithm

While adopting the algorithm used in papers I and II, some issues arose, which might impact the quality and quantity of results obtained.

Missing passes

It was found that the code only correctly implemented the forward pass of the algorithm. Because of incorrectly calculating the window ranges for the backwards and shifted passes, these were not actually implemented. We

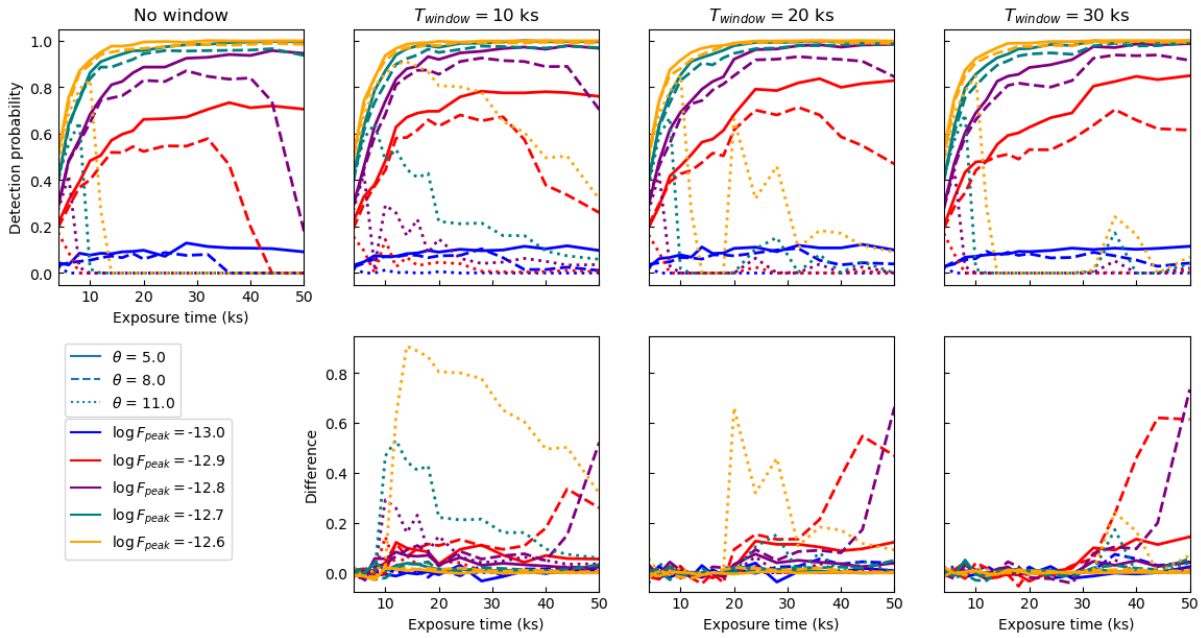

Figure 2.1 Detection probability for the search algorithm, using a range of window sizes. The first row displays the absolute detection probability. The second row displays the difference in probability to the algorithm not utilising windows. The different color lines represent the peak flux levels. The different line styles represent the off-axis angles. It is not immediately obvious one window sizes is more suitable than others. This suggests, it might be worthwhile to undertake searches using a number of other window sizes.

ran a 20 ks search on all data, only using the forward pass to see the effect of this change. The results of this test can be found in section 3.1.3.

Limiting residual window sizes

While visually checking preliminary results, we saw many detections originating from the residual window. Almost all of these detections had in common that they had no visually noticeable variability in counts. So, they should not have been picked up by the algorithm. This happened because the residual windows of these detections were too small. This caused large variability due to noise, subsequently leading to a false positive detection. To fix this we implement a minimum window size of 8 ks. This is the same limit papers I and II imposed on the overall exposure time, because the detection probability decreases greatly for observations below 8 ks.

2.3 Data Selection

All observation analysed in this thesis were publicly released in the period from 1999-09-04, to 2024-05-21 and are obtained from the Chandra Data Archive using the `download_chandra_obsid` `CIAO` tool. We use the same data constraints as discussed in section 2.3 of paper II, which are as follows. Only Chandra Advanced CCD Imaging Spectrometer (ACIS) Data is considered. We specifically look at extragalactic transients. So, we would like to eliminate as many Galactic sources as possible. A limit of $|b| > 10^1$ is chosen to eliminate much of the Galactic disk and thus many of the Galactic sources. Furthermore, exposure time is limited to 8 ks at a minimum.

[1] b being the angle relative to the Galactic disk.

2.4 Generation of light curves

We generate light curves of every source within an observation by first extracting every source from the event file using the `wavdetect` tool from the `CIAO` data analysis tool. The `wavdetect` tool first correlates a given image with wavelets of different sizes then searches these results for significant correlations. In addition to the coordinates, `wavdetect` gives us the positional error of the source coordinates, from here on mentioned as σ and the signal to noise ratio of the source. The light curve of a source is constructed by taking the source coordinates given by this procedure and excluding all events in the event files that fall outside a $1.5 \times R_{90}$ radius of the source. Where R_{90} is the radius encompassing 90% of x-ray counts, which is a function of the off-axis angle of a source. To compensate for the background radiation, we take an annulus around the source with an inner radius equal to that of the source and an outer radius of $1.5 \times R_{90} + 20$ pixels. The number of background counts in the annulus is then compensated by the ratio of the source area to the annulus area to get the estimated number of background counts in the source.

It is important to note that this method of light curve generation differs from that of paper I, in which only sources present in the CSC2 catalog were analysed. Consequently, we expect to obtain more detections in this period, as the CSC2 catalog has a much higher threshold for its sources.

2.5 Filtering

In this section we discuss how we filter the list of FXT detections to reject non FXT sources. The filtering is performed across four criteria: archival x-ray data (Sect. 2.5.1), stellar objects with the GAIA catalog (Sect. 2.5.2) and more Galactic objects with NED, SIMBAD and VIZIER (Sect. 2.5.3). The remaining detections are checked for variability (Sect. 2.5.4 and manual filtered (Sect. 2.5.5). It is important to note that a boresight correction of 0.5 arcseconds is added to all mentioned search radii (CXC, 2024a).

2.5.1 Criterion I: Archival X-ray data

FXTs are by definition only observed once. To check if a detection is indeed of transient nature we have to check for prior and subsequent detections of the same source. To do this we use the `search_csc` `CIAO` tool to query the CSC2.1 Chandra catalog (Evans et al., 2010) for additional observations of the same source. We use the `astroquery` Python package (Ginsburg et al., 2019) to query archival x-ray data of the XMM-Newton, Swift, ROSAT and Erosita missions (Webb et al., 2020; Evans et al., 2014; Evans et al., 2020; Boller et al., 2016; Tubín-Arenas et al., 2024). Furthermore, we use a catalog of x-ray binaries (Kovlakas et al., 2020) to eliminate objects of this nature, since we are not interested in objects previously classified as x-ray binaries.

For Chandra we require non-detections at 3σ confidence level and use a search radius of 3σ. For the other catalogs we require a non-detection in a 5σ search radius. This higher threshold is due to the sharper point spread function (PSF) of Chandra relative to other telescopes like XMM-Newton. (Weisskopf et al., 2000; Jansen, F. et al., 2001). The PSF describes the shape and size of an image produced by a point source. Thus, a sharper or lower PSF allows us to more accurately measure the position of sources.

2.5.2 Criterion II: GAIA stellar catalog

Since we look for extragalactic FXTs we can use the GAIA catalog (Gaia Collaboration, 2016; Gaia Collaboration et al., 2022) to discard a large number of Galactic stellar sources. We use the same search radius of 3σ around our FXT detections and we require any match we obtain to have a non-zero proper motion[2]. This signifies the source is Galactic, since it is close enough to us, to have an observable non-zero proper motion.

2.5.3 Criterion III: NED SIMAD VIZIER

To further eliminate galactic detections we will use the NED and SIMBAD catalogs (Helou et al., 1991; Wenger et al., 2000), as well as Wang et al. (2020), Lawrence et al. (2007), Ahumada et al. (2020), and McMahon et al. (2013). We again use the `astroquery` Python package via the Vizier catalog library (Ochsenbein, Bauer, and Marcout, 2000), to query these catalogs with a search radius of 3σ.

2.5.4 Criterion IV: Probability of Variability

Even with the strict requirements for a source to be marked as a detection, many sources which do not have an apparent variability are still detected. These sources, in a way, "get lucky". That is to say, a certain window of the algorithm falls in such a way, that it precisely picks up a peak in the seemingly random and noisy data. The algorithm does not look at the rest of the observation when considering one particular window. So, the algorithm cannot differentiate between a random peak and a real flash.

To try and eliminate these kinds of detections we use the Gregory Loredo algorithm (G-L). This is implemented in the `glvary` `CIAO` tool. Supplying the light curve and source data, the algorithm calculates a probability of it being a variable source. We discard any source with a probability lower than one half. Any source with a higher value may be variable so will not be discarded. In paper II this criterion discarded one candidate that had passed the previous filters.

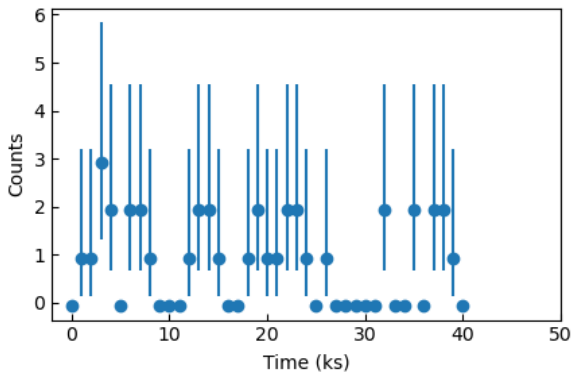

Figure 2.2 Example of a light curve rejected by the G-L algorithm. This source was detected in observation 16302, at 209.0045 -32.5877 (deg). No clear transient event is present in this light curve.

[2]The movement a source has relative to the background of distant stars.

2.5.5 Criterion IV: Manual filtering

Once a detection is through all previous steps it remains to be checked manually. This is outside the scope of this thesis due to the large number of new candidates found. However, while inspecting images of one observation, it was discovered to have a number of detections due to an instrumental effect. This case is further discussed in section 3.1.1 and the general process of manual filtering is discussed in sections 2.7.4 and 2.7.5 in paper II.

Chapter 3

Results

In this section we discuss the results obtained from the method described in chapter 2. We separate this chapter into the results for the 20 ks window size (Sect. 3.1) and for the 50 ks window size (Sect. 3.2).

3.1 20ks

While our main goal is to find longer FXTs then currently found, we do a 20 ks search in addition. Beside checking the results of our implementation against those of papers I and II, there are three other reasons why this search is not unnecessary.

As mentioned in section 2.4 the method of source extraction had changed from paper I to paper II. Possibly increasing the number of sources to analyse in the paper I period. Second, since the release of paper II, new data has been released which remains to be analysed. Third, as described in section 2.2.2, an error was found in the implementation of the algorithm in the previous papers. The effect of this issue is discussed in section 3.1.3.

Table 3.1 Breakdown of the 20 ks window search in the periods of paper I, paper II and new data.

	Total	Paper I	Paper II	New Data
Observations	9799	4992	3311	1496
Analysed	9634	4834	3304	1496
Detections	1301	1050	206	45
Candidates	47	35	10	2

Notes: Total: All Chandra data. Paper I: From beginning of Chandra observations to 2015-01-01. Paper II: From 2015-01-01 to 2022-04-01. New Data: From 2022-04-01 to 2024-05-20.

In table 3.1 a breakdown of the 20ks search can be seen. The number of observations and number of analysed observations is different for the periods of papers I and II. This is due to some observations encountering errors in downloading or light curve generation.

3.1.1 Old Data

Papers I and II obtained 728 and 151 detections respectively. As seen in tables 3.2 and 3.3 we have obtained 1050 and 206 respectively. We mention two factors which could possibly cause this difference. First, the change in light curve extraction from paper I to paper II and our implementation, discussed in section 2.4. Second, the change in the implementation of the search algorithm, discussed in section 2.2.2.

Table 3.2 The filtering process for the 20 ks search of the paper I data. Starting with 1050 detections.

Criterion	Matched	Rate	Unique	Removed	Remaining
Archival X-ray date	778	74%	65	778	272
Cross-match with stars/Gaia	710	68%	56	173	99
NED + SIMBAD + VizieR	746	71%	28	32	63
Prob. of variability	-	-	-	11	52
Manual	-	-	-	17	35

Notes: Matched: The number of detections with a match in the criterion. Rate: Ratio of total detections to number of matched detections. Unique: The number of detections with a match only in this criterion. Removed: The number of detections thrown out when applying the criteria in order. Remaining: The number of remaining detections after applying the criterion.

Table 3.3 The filtering process for the 20 ks search of the paper II data. Starting with 206 detections.

Criterion	Matched	Rate	Unique	Removed	Remaining
Archival X-ray date	143	69%	13	143	61
Cross-match with stars/Gaia	142	69%	19	45	16
NED + SIMBAD + VizieR	123	60%	3	4	12
Prob. of variability	-	-	-	2	10

One observation was eliminated due to instrumental effects. This was noticed while inspecting the image of the observation as seen in 3.1. A bright line can be clearly seen in the image. All 17 candidates of this observation fall on this line, which is caused by a readout streak (CXC, 2024b). These candidates can thus be discarded. No further manual filtering was done, so only table 3.2 has data for this step.

In total we have found 35 and 10 candidates across the period of papers I and II respectively. All but two of the previously found FXTs have been found by our implementation. The first being XRT 161125. The exposure time of the Chandra observation this FXT is found in is below the minimum of 8 ks, so it was not analysed. The second being XRT 210423. The source this FXT originates from was not extracted with `wavdetect`. However, by testing the algorithm on its coordinates manually, it did correctly identify the FXT. What causes this issue with the `wavdetect` tool is unclear. Consequently, we can not be sure whether or not more sources were missed.

The number of candidates before manual checking was 29 and 9 for papers I and II respectively. It is unclear whether all of the previously found candidates have been found by our implementation, since only the final list of FXTs was published. Hence, we cannot precisely say how many new candidates are found. However, if we were to assume all candidates in papers I and II were also found by our implementation, we would be left with 6 and 3 new candidates not found before. The manual filtering step, does not fall within the scope of this thesis. Hence, we will not discuss these FXT candidates any further. Their properties and light curves can be found in appendix A.

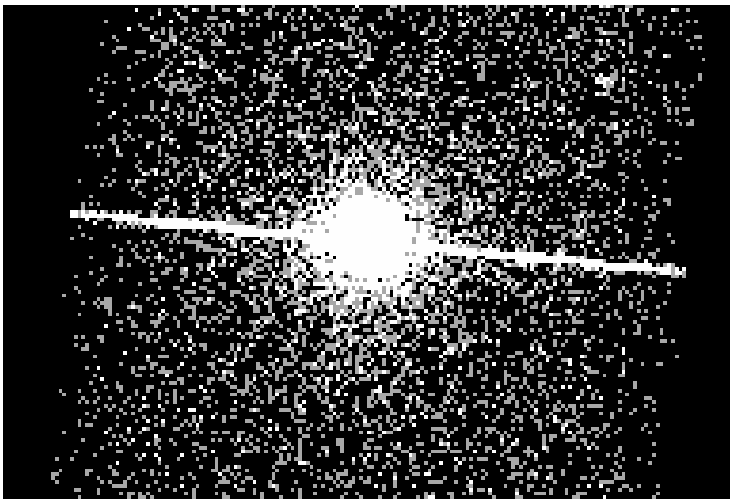

Figure 3.1 A zoomed in image of the event file for Chandra ObsID 2561. The bright source is object CD-23 14742. The bright line seen across the image is the result of a so called readout streak (CXC, 2024b). Because of the instrumental error, all sources in this observation were excluded from the list of candidates.

3.1.2 New Data

From the period of new data we obtained 45 detections. Of these, only two detections passed all filters. As seen in table 3.4. Both of these two candidates also passed the variance check described in section 2.5.4. The properties of these candidates can be found in table 3.5 and the light curves of these candidates can be found in figure 3.2.

Table 3.4 The filtering process for the 20 ks search of the new data. Starting with 45 detections.

Criterion	Matched	Rate	Unique	Removed	Remaining
Archival X-ray date	20	44%	2	20	25
Cross-match with stars/Gaia	28	62%	10	19	6
NED + SIMBAD + VizieR	20	44%	2	4	2
Prob. of variability	-	-	-	-	-

Notes: See table 3.2 for column definitions.

3.1.3 Implementation error

We performed a 20 ks search using only the forward pass, to test the effect of the implementation error discussed in section 2.2.2. The results of this search can be seen in table 3.6.

In total we had 65% less detections and 43% less candidates across the whole data set. Implementing the backward and shifted passes seems to make a significant difference in the number of sources detected and subsequently marked as candidates.

Table 3.5 Candidates found in the new data with a 20 ks window.

	Id	ObsId	Exp. (ks)	Date	T_{90}	RA (deg)	Dec (deg)	Off. Ang.	Pos. Unc.	S/N
	(1)	(2)	(3)	(4)	(5)	(6)	(7)	(8)	(9)	(10)
1	XRTC 210515	23488	29.6	2021-05-15	$25.0^{+3.3}_{-10.3}$	187.66173	41.63609	$2.5'$	$0.18''$	28.1
2	XRTC 231009	28964	12.4	2023-10-09	$2.0^{+0.2}_{-0.7}$	244.71650	−1.99187	$6.1'$	$0.72''$	5.7

Notes: (1): FXT Id being the date on which the Chandra observation of the candidate ended. (2): Chandra observation Id. (3): Exposure time of Chandra observation. (4): Start and end date of Chandra observation. (5): T_{90} of the FXT candidate. (6): Right ascension of the source. (7): Declination of the source. (8): Angle from center of Chandra observation axis to the source. (9): Positional uncertainty in the source position. (10): Signal to noise ratio of the source.

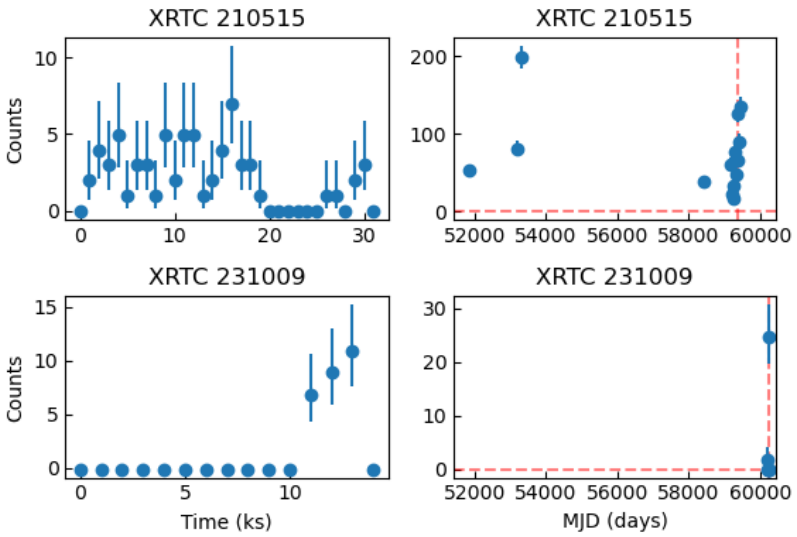

Figure 3.2 Short and long term light curves of every candidate found by the 20 ks search. Column 1: The light curve of the observation the detection was found in, as a relation of counts against time in kiloseconds. Column 2: The long term light curve of the total number of counts in every observation of the same source in the CSC2.1 catalog, as a relation of counts against time in days. The vertical dashed line represents the time of the observation the candidate was found in. The horizontal dashed line represents zero counts.

3.2 50ks

The algorithm found five new FXT candidates which had not been found in previous searches or in the 20 ks search discussed in section 3.1.

In table 3.7 we see the numbers of analysed observations in each period is much lower than that of the 20 ks search. For other searches than 20ks only observations longer than the window size were considered, as the entire observation would already have been analysed in the 20 ks search. Additionally, we can see a rapid decrease in the numbers of analysed, detections and candidates. This might be attributed to the decrease of long Chandra observations in more recent periods, which can be seen in figure 3.3.

Table 3.6 Breakdown of the 20 ks window search, using only the forward pass in the periods of paper I, paper II and new data.

	Total	Paper I	Paper II	New Data
Observations	9799	4992	3311	1496
Analysed	9634	4834	3304	1496
Detections	456	328	93	35
Candidates	27	19	7	1

Table 3.7 Breakdown of the 50 ks window search in the periods of paper I, paper II and new data.

	Total	Paper I	Paper II	New Data
Observations	9799	4992	3311	1496
Analysed	973	716	251	6
Detections	615	549	66	0
Candidates	40	37	3	0

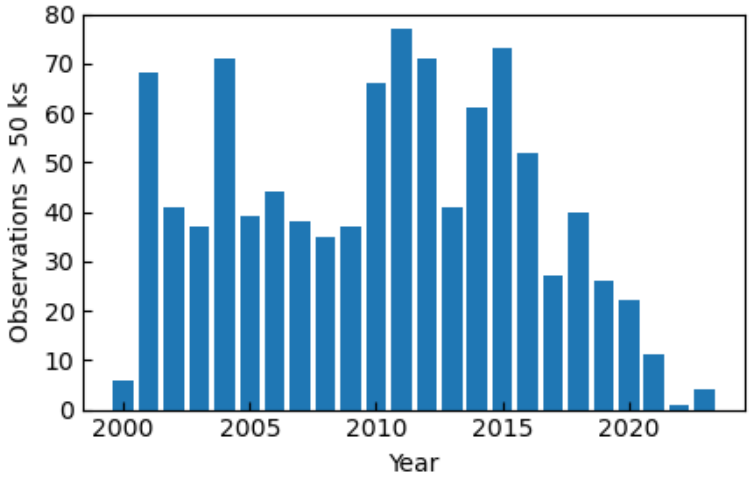

Figure 3.3 The number of observations with an exposure time greater than 50 ks per year, within all analysed observations in this work. We can see a drop off starts to occur around 2015 which roughly coincides with the start of the paper II period. This explains the reduction of analysed observations, seen in table 3.7, across the different periods.

Table 3.8 The filtering process for the 50 ks search of the new data. Starting with 615 detections.

	Matched	Rate	Unique Matched	Removed	Remaining
Archival X-ray date	474	77%	46	474	141
Cross-match with stars/Gaia	389	63%	36	78	63
NED + SIMBAD + VizieR	438	71%	19	20	40
Prob. of variability	-	-	-	-	-

Table 3.9 Candidates found by the 50ks pass, which have not been found in the 20ks pass.

	Id	ObsId	Exp. (ks)	Date	T_{90} (ks)	RA (deg)	Dec (deg)	Off. Ang.	Pos. Unc.	S/N
1	XRTC 001204	1882	96.8	2000-12-02/ 2000-12-04	$70.0^{+7.4}_{-11.1}$	91.94792	−6.39343	1.0′	0.18″	15.1
2	XRTC 030120	4396	164.6	2003-01-18/ 2003-01-20	$45.2^{+44.4}_{-20.4}$	83.84385	−5.33084	4.1′	0.15″	44.9
3	XRTC 060530	6792	97.3	2006-05-29/ 2006-05-30	$90.5^{+4.1}_{-17.9}$	221.89159	9.33420	6.0′	0.85″	9.7
4	XRTC 100819	12301	78.0	2010-08-18/ 2010-08-19	$58.7^{+3.0}_{-8.6}$	148.88870	68.96563	3.2′	0.42″	7.1
5	XRTC 110501	12317	78.5	2011-04-30/ 2011-05-01	$76.6^{+3.5}_{-4.9}$	191.86629	−2.15688	0.6′	0.12″	33.2

Notes: See table 3.5 for column definitions.

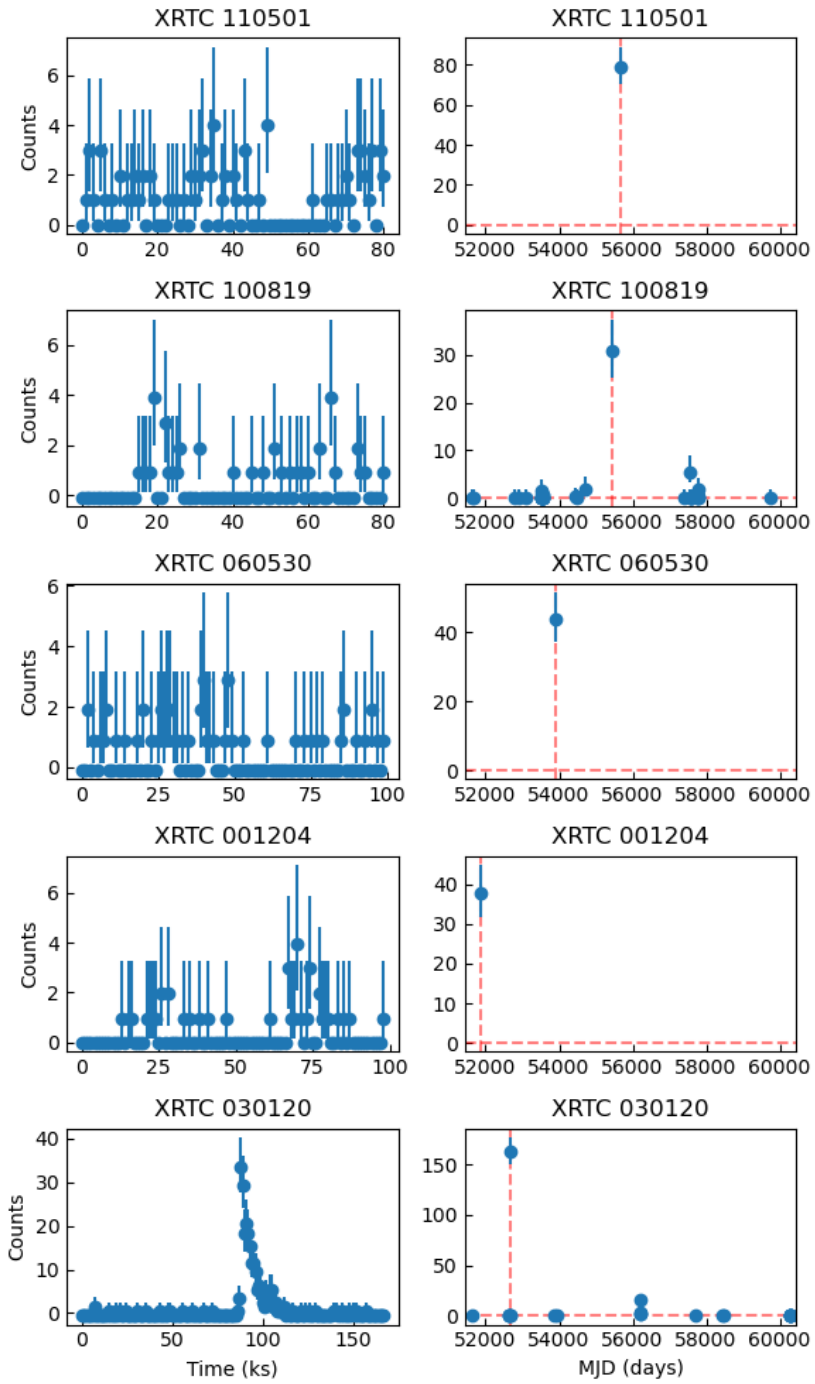

Figure 3.4 Short and long term light curves of every candidate found by the 50 ks search. See figure 3.2 for column definitions.

Chapter 4

Conclusion and further research

Out of 9634 observation from 2000-02-03 to 2024-05-20 we have found 47 FXT candidates, using a 20 ks window size. Of these, 45 are in the period of papers I and II and two in the period after. In the same time period we have also found five new candidates using a window size of 50 ks.

Twenty of these candidates are previously identified in papers I and II. It is likely, most of the candidates have been identified previously as well but later manually rejected.

Papers I and II identified in total 38 candidates before manual filtering. Two of the final FXTs were not identified in this thesis and it is unknown what fraction of our candidates is part of these previous candidates. However, assuming all remaining 36 are part of our sample of 45, we would have a minimum of 9 new candidates.

It remain to be manually confirmed, whether or not these candidates are actual FXTs. Because of this, we can not make any definitive statements about the data, but we can say something about their effect, should they be confirmed. If a larger than zero fraction of these candidates is confirmed, the FXT event rate would of course increase with respect to previously reported values. This would also affect the likelihood of possible origins of FXTs. This depends on the event rate among many other parameters. Additionally, whether the 50ks candidates are confirmed to be FXTs is very important to our understanding of the idea that the FXTs could originate from off-axis gamma ray burst afterglow (Wichern et al., 2024).

4.1 Further research

Since this subject is still in its infancy, there is much to be discovered about FXTs. The process developed in papers I and II and built upon in this thesis can still be improved and expanded in two main areas. First, the simulation in 2.2.1 showed there to be not much difference in detection probabilities of the different window sizes. Searches of additional window sizes could therefore yield even more candidates yet to be identified. This has also become easier with the help of the framework developed in this thesis. Which aimed to make the method used in papers I and II more adaptable.

Second, this thesis covers all observations publicly released up to the 20th of April, 2024. However, new data is still being published. Ideally, the algorithm would be run continuously, analysing every new observation as it is released. Finding new candidates within these observations is crucial in finding out more about their origins. Discovering a recent FXT might allow us to detect multiwavelength emissions still present after the initial event. In

the case of Chandra, these FXTs can be identified up to two decades after the event took place. This makes it hardly possible to detect multiwavelength counterparts, which has only been possible in one instance, namely for XRT 080109/SN 2008D (Mazzali et al., 2008; Soderberg et al., 2008; Modjaz et al., 2009).

Appendix A

Candidate Properties and Light Curves

In this appendix are all the properties and light curves of the candidates found in the 20ks search which were not displayed earlier.

Table A.1 List of FXT candidates found by the 20ks search in the period of paper I.

	Id	ObsId	Exp. (ks)	Date	T_{90} (ks)	RA (deg)	Dec (deg)	Off. Ang.	Pos. Unc.	S/N
1	XRT 000519	803	28.5	2000-05-19	$15.8^{+1.8}_{-1.6}$	186.38158	13.06645	$13.3'$	$0.46''$	107.9
2	XRTC 010809	1878	75.5	2001-08-08/ 2001-08-09	$56.2^{+9.3}_{-11.6}$	85.43966	−1.90754	$0.8'$	$0.08''$	51.4
3	XRTC 010809	1878	75.5	2001-08-08/ 2001-08-09	$58.7^{+8.4}_{-31.4}$	85.45288	−1.90446	$1.0'$	$0.29''$	12.4
4	XRTC 010809	1878	75.5	2001-08-08/ 2001-08-09	$25.7^{+1.2}_{-1.4}$	85.44771	−1.92406	$0.3'$	$0.04''$	278.2
5	XRTC 001204	1882	96.8	2000-12-02/ 2000-12-04	$57.3^{+23.2}_{-13.3}$	91.90500	−6.38148	$3.4'$	$0.21''$	25.8
6	XRTC 001204	1882	96.8	2000-12-02/ 2000-12-04	$54.4^{+39.4}_{-19.1}$	91.89683	−6.38541	$3.9'$	$0.32''$	8.0
7	XRTC 001204	1882	96.8	2000-12-02/ 2000-12-04	$76.2^{+2.4}_{-12.3}$	91.94014	−6.38184	$1.3'$	$0.24''$	10.9
8	XRTC 001204	1882	96.8	2000-12-02/ 2000-12-04	$54.0^{+10.3}_{-16.5}$	91.94413	−6.37715	$1.1'$	$0.11''$	28.0
9	XRTC 021001	2736	65.2	2002-09-30/ 2002-10-01	$18.3^{+10.3}_{-17.7}$	6.04418	−72.09146	$0.6'$	$0.16''$	8.9
10	XRTC 020713	3184	87.5	2002-07-12/ 2002-07-13	$60.0^{+6.1}_{-9.8}$	104.40282	−55.81076	$8.7'$	$1.22''$	10.9

Notes: See table 3.5 for column definitions.

Table A.2 Continuation of table A.1.

	Id	ObsId	Exp. (ks)	Date	T_{90}	RA (deg)	Dec (deg)	Off. Ang.	Pos. Unc.	S/N
11	XRTC 020518	3214	14.9	2002-05-18	$9.0^{+3.7}_{-1.3}$	238.11094	20.19988	$4.9'$	$0.70''$	14.6
12	XRTC 030122	3498	69.0	2003-01-21/ 2003-01-22	$41.0^{+15.3}_{-21.0}$	83.82902	−5.47276	$4.7'$	$0.77''$	7.3
13	XRTC 030112	3744	164.2	2003-01-10/ 2003-01-12	$142.4^{+7.7}_{-9.9}$	83.62232	−5.39870	$11.8'$	$0.00''$	68.3
14	XRT 030511	4062	46.1	2003-05-10/ 2003-05-11	$14.5^{+9.8}_{-6.0}$	76.77818	−31.86982	$10.7'$	$0.74''$	41.9
15	XRTC 030117	4374	169.0	2003-01-15/ 2003-01-17	$113.6^{+84.9}_{-29.9}$	83.77555	−5.38505	$2.7'$	$0.25''$	9.9
16	XRTC 030120	4396	164.6	2003-01-18/ 2003-01-20	$53.3^{+41.5}_{-7.9}$	83.88027	−5.37104	$3.9'$	$0.38''$	13.8
17	XRTC 040802	5353	36.6	2004-08-01/ 2004-08-02	$29.2^{+1.4}_{-10.6}$	329.12392	−4.83024	$4.0'$	$0.51''$	6.9
18	XRTC 040802	5353	36.6	2004-08-01/ 2004-08-02	$34.0^{+0.1}_{-1.4}$	329.14680	−4.86583	$5.4'$	$0.84''$	3.9
19	XRT 041230	5885	70.7	2004-12-30/ 2004-12-31	$30.9^{+3.0}_{-17.8}$	318.12660	−63.49898	$3.7'$	$0.42''$	8.8
20	XRTC 060706	6436	36.5	2006-07-05/ 2006-07-06	$23.0^{+5.7}_{-9.7}$	52.24340	31.37147	$1.6'$	$0.12''$	38.6
21	XRTC 060706	6436	36.5	2006-07-05/ 2006-07-06	$25.3^{+0.9}_{-2.2}$	52.28227	31.36582	$1.3'$	$0.22''$	20.6
22	XRTC 070612	7439	34.1	2007-06-11/ 2007-06-12	$16.3^{+6.3}_{-9.8}$	296.11682	50.58232	$4.6'$	$0.53''$	12.9
23	XRT 080819	9841	15.8	2008-08-19	$8.4^{+1.6}_{-3.9}$	175.00503	−31.91742	$4.7'$	$0.73''$	10.5
24	XRTC 090301	9923	14.7	2009-03-01	$7.8^{+1.0}_{-3.6}$	193.92558	38.35555	$4.5'$	$0.68''$	5.8
25	XRTC 081224	10234	31.7	2008-12-24	$25.8^{+2.5}_{-2.5}$	59.83881	10.47411	$7.1'$	$0.93''$	10.4
26	XRTC 100914	11737	52.3	2010-09-14	$31.1^{+0.4}_{-26.1}$	337.78288	39.37290	$1.6'$	$0.24''$	8.0
27	XRTC 100101	11777	29.2	2010-01-01	$24.0^{+1.0}_{-2.3}$	138.08401	35.05535	$1.9'$	$0.13''$	44.4
28	XRT 100831	12264	40.0	2010-08-31	$8.6^{+0.9}_{-4.8}$	90.00443	−52.71504	$4.7'$	$0.55''$	12.1
29	XRTC 111009	12273	9.9	2011-10-08/ 2011-10-09	$7.2^{+1.6}_{-1.5}$	87.16240	−25.56932	$5.6'$	$0.75''$	9.9
30	XRTC 111003	12315	39.2	2011-10-02/ 2011-10-03	$28.3^{+2.0}_{-3.1}$	36.43187	12.87232	$1.4'$	$0.11''$	49.1
31	XRT 110103	12884	84.5	2011-01-03/ 2011-01-04	$60.9^{+10.3}_{-8.9}$	212.12047	−27.05800	$13.0'$	$0.81''$	33.7
32	XRT 110919	13454	91.8	2011-09-19/ 2011-09-20	$64.1^{+12.0}_{-29.3}$	15.93569	−21.81271	$7.4'$	$0.65''$	16.7
33	XRT 130822	14904	29.7	2013-08-22	$14.4^{+3.4}_{-4.0}$	345.49250	15.94870	$1.6'$	$0.17''$	13.4
34	XRT 140327	15113	33.6	2014-03-27	$15.4^{+0.7}_{-5.6}$	45.26836	−77.88092	$6.6'$	$1.30''$	7.6
35	XRT 141001/ CDF-S XT1	16454	47.1	2014-10-01	$5.0^{+10.0}_{-3.0}$	53.16163	−27.85949	$3.7'$	$0.17''$	47.1

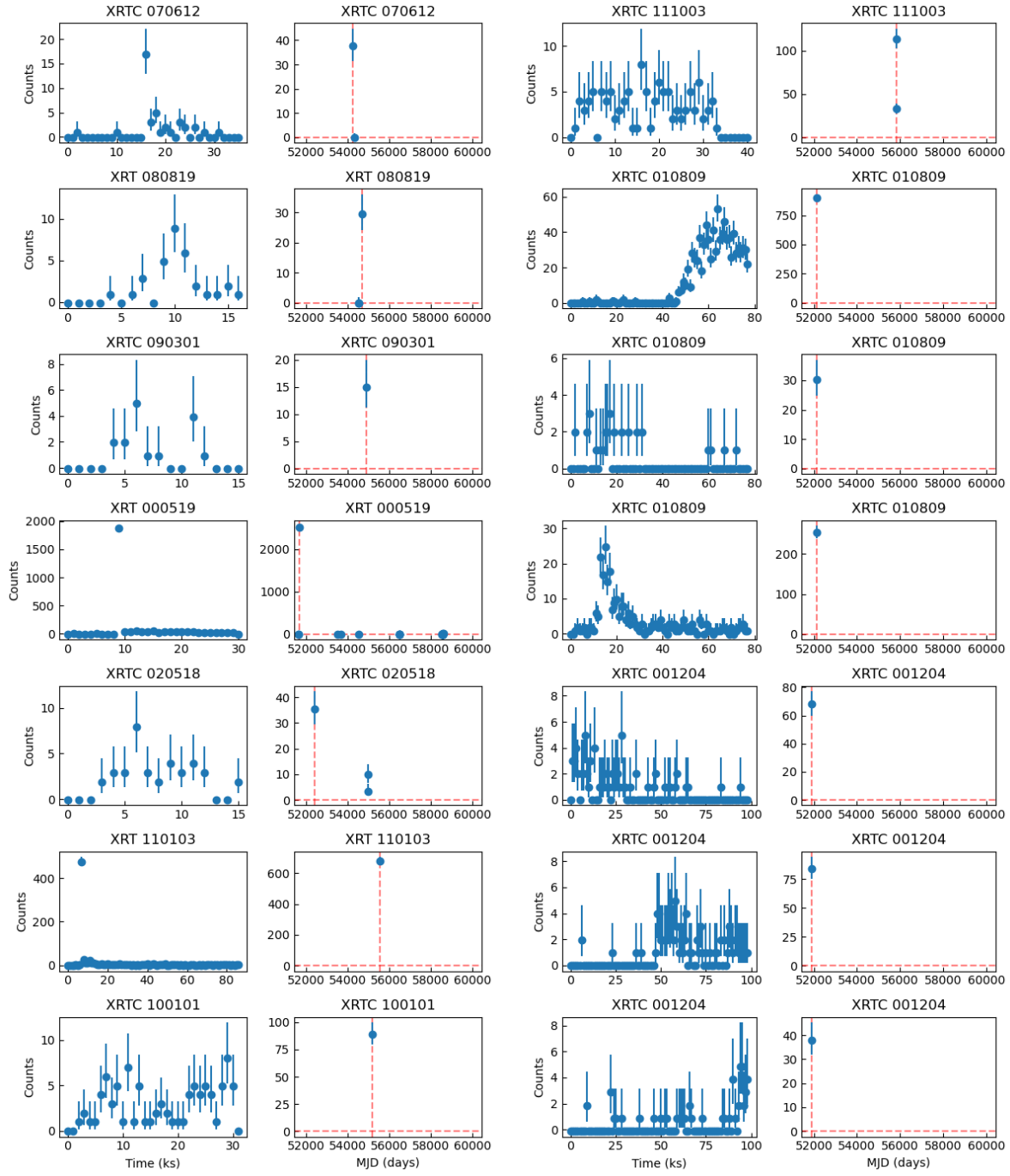

(a) 1 - 7 *(b)* 8 - 14

Figure A.1 Short and long term light curves of every candidate found in the period of paper I, split into two figures. See figure 3.2 for column definitions.

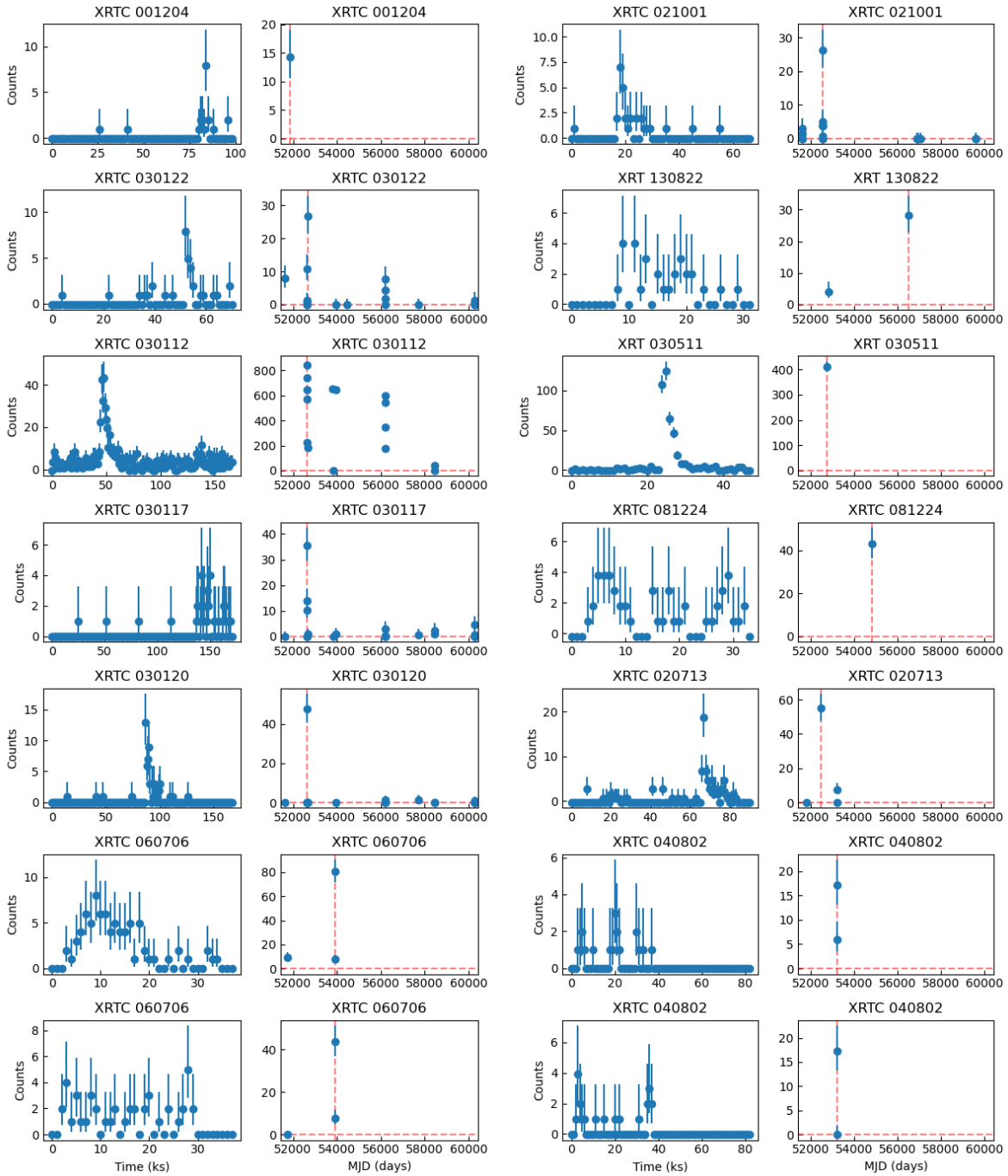

(a) 15 - 21 *(b)* 21 - 28

Figure A.2 Continuation of figure A.1.

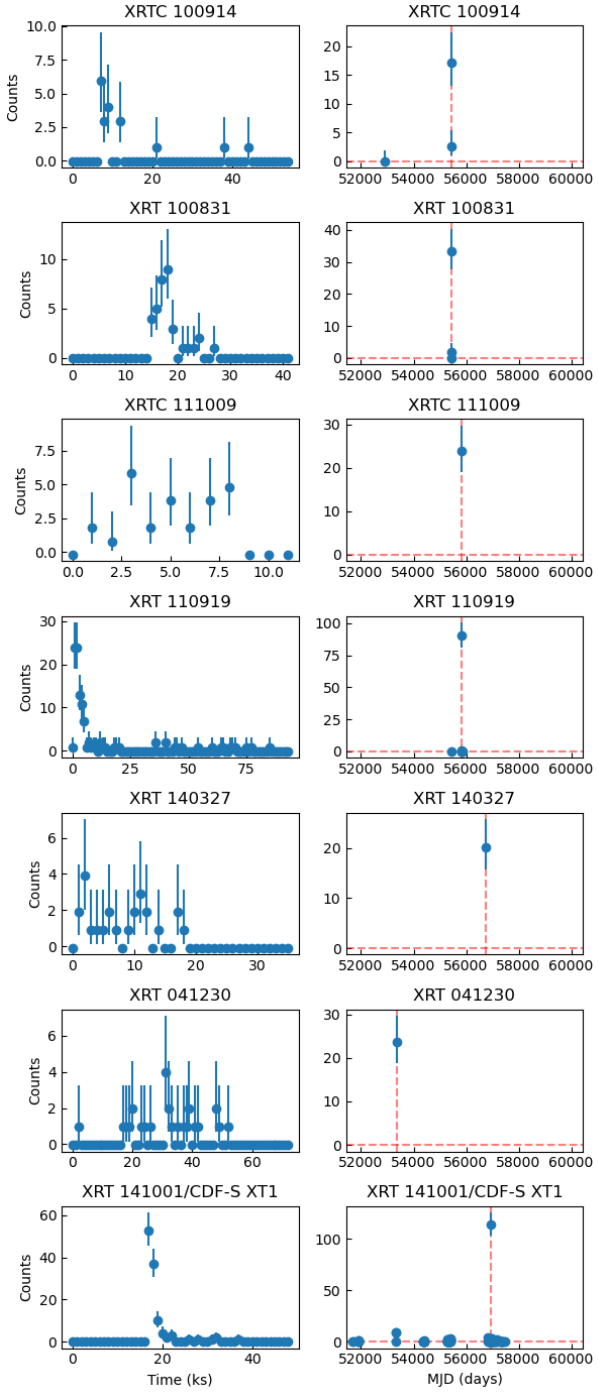

Figure A.3 Continuation of figure A.2.

Table A.3 List of FXT candidates found by the 20ks search in the period of paper II.

	Id	ObsId	Exp. (ks)	Date	T_{90} (ks)	RA (deg)	Dec (deg)	Off. Ang.	Pos. Unc.	S/N
1	XRT 140507	16093	66.7	2014-05-07	$4.8^{+3.5}_{-5.5}$	233.73481	23.46840	$2.2'$	$0.33''$	9.6
2	XRT 150322/ CDF-S XT2	16453	70.3	2015-03-21/ 2015-03-22	$10.5^{+7.7}_{-5.8}$	53.07676	−27.87361	$4.3'$	$0.24''$	45.7
3	XRTC 161209	17615	26.3	2016-12-08/ 2016-12-09	$19.2^{+3.6}_{-7.3}$	207.61486	26.74966	$4.7'$	$0.82''$	10.6
4	XRTC 161209	17615	26.3	2016-12-08/ 2016-12-09	$24.0^{+1.7}_{-7.6}$	207.62469	26.69989	$2.0'$	$0.29''$	6.5
5	XRT 151121	18715	21.8	2015-11-20/ 2015-11-21	$17.9^{+12.3}_{-0.6}$	40.82961	32.32377	$8.6'$	$1.83''$	9.0
6	XRTC 171213	18927	37.4	2017-12-13	$6.1^{+2.3}_{-2.5}$	83.87398	−4.99735	$0.2'$	$0.26''$	11.9
7	XRT 170901	20635	74.2	2017-08-31/ 2017-09-01	$4.2^{+0.9}_{-0.8}$	356.26459	−42.64493	$3.1'$	$0.14''$	61.8
8	XRT 191127	21831	19.8	2019-11-26/ 2019-11-27	$0.5^{+0.2}_{-12.1}$	207.34719	26.58445	$5.9'$	$0.85''$	11.7
9	XRTC 200413	22558	19.8	2020-04-12/ 2020-04-13	$7.4^{+0.8}_{-6.9}$	289.58998	49.60696	$4.2'$	$0.30''$	43.5
10	XRT 191223	23103	16.4	2019-12-23	$3.7^{+0.6}_{-1.8}$	50.47529	41.24683	$3.5'$	$0.46''$	10.7

Notes: See table 3.5 for column definitions.

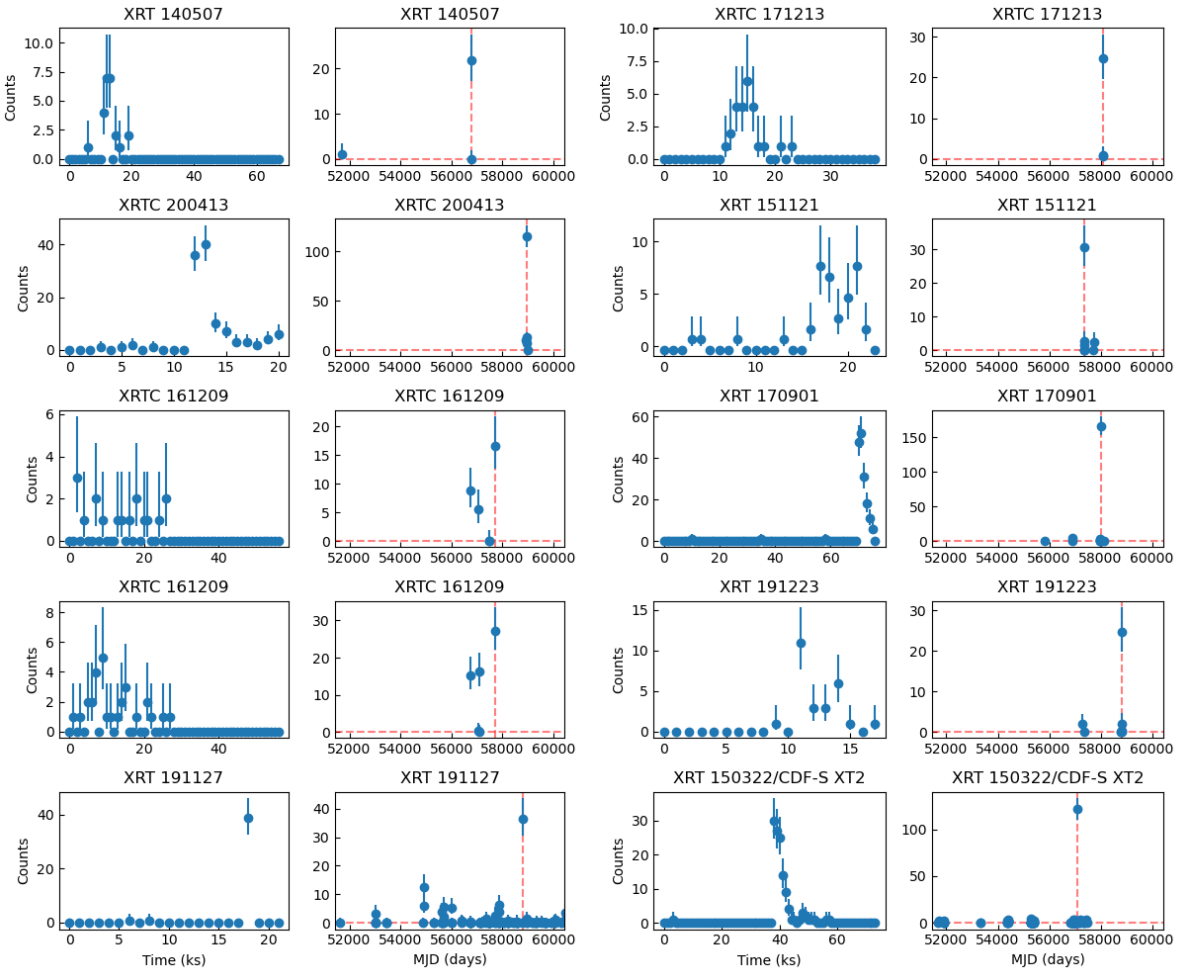

(a) The first six candidates.

(b) The last six candidates.

Figure A.4 Short and long term light curves of every candidate found in the period of paper II, split into two figures. See figure 3.2 for column definitions.

Appendix B

Research data management

All data downloaded from all mentioned third party sources, generated by the process and generated for this thesis in the form of tables and figures, was stored on the dedicated FXT research server in the Astrophysics department of Radboud University.

The implementation of the algorithm and filter criteria, as well as the code to calculate candidate properties and generate candidate tables and light curve figures, can be found in the GitHub repository for this thesis. A list of all searched Chandra Obs IDs can also be found in this repository.

B.1 Calculations

This section mentions the method of obtaining and calculating the figures seen in tables 3.5, 3.9, A.1, A.2 and A.3. The right ascension, declination, off-axis angle, positional uncertainty and signal to noise ratio are all calculated by the `wavdetect` tool. The T_{90} time is the time between the light curve reaching 5% of its total counts and reaching 95% of its total counts. This is obtained by first calculating the beginning and ending times of the FXT candidate. We do this in bins of 100 seconds and take the first and last instances a bins counts are greater than five times the background level, obtained as described in section 2.4. We then calculate the time at which the reduced light curve reaches 5% and 95% of its counts, giving the T_{90}. In papers I and II, counts are assumed to be Poisson distributed, the upper and lower errors on the T_{90} are thus calculated as follows. First, upper and lower errors are calculated on the 5% and 95% number of counts. This is done with the `astropy` Python library (Astropy Collaboration et al., 2013; Astropy Collaboration et al., 2018; Astropy Collaboration et al., 2022). These upper and lower counts are again mapped to the time at which the light curve reaches these values, which gives the upper and lower errors for T_{90}.

Bibliography

Bauer, Franz E. et al. (June 2017). “A new, faint population of X-ray transients”. In: *mnras* 467.4. _eprint: 1702.04422, pp. 4841–4857. DOI: 10.1093/mnras/stx417.

Quirola-Vásquez, J. et al. (July 2022). “Extragalactic fast X-ray transient candidates discovered by Chandra (2000-2014)”. In: *Astronomy and Astrophysics* 663. Publisher: EDP Sciences. DOI: 10.1051/0004-6361/202243047.

Quirola-Vásquez, J. et al. (July 2023). “Extragalactic fast X-ray transient candidates discovered by Chandra (2014-2022)”. In: *Astronomy and Astrophysics* 675. Publisher: EDP Sciences. DOI: 10.1051/0004-6361/202345912.

Waxman, Eli and Boaz Katz (2017). “Shock Breakout Theory”. In: *Handbook of Supernovae*. Ed. by Athem W. Alsabti and Paul Murdin, p. 967. DOI: 10.1007/978-3-319-21846-5_33.

Jonker, P. G. et al. (Dec. 2013). “Discovery of a New Kind of Explosive X-Ray Transient near M86”. In: *apj* 779.1. _eprint: 1310.7238, p. 14. DOI: 10.1088/0004-637X/779/1/14.

Glennie, A. et al. (July 2015). “Two fast X-ray transients in archival Chandra data”. In: *mnras* 450.4. _eprint: 1504.03720, pp. 3765–3770. DOI: 10.1093/mnras/stv801.

Wichern, H. et al. (July 2024). *Investigating the off-axis GRB afterglow scenario for extragalactic fast X-ray transients*.

Yang, G. et al. (June 2019). “Searching for fast extragalactic X-ray transients in Chandra surveys”. In: *Monthly Notices of the Royal Astronomical Society* 487.4. Publisher: Oxford University Press, pp. 4721–4736. DOI: 10.1093/mnras/stz1605.

Fruscione, Antonella et al. (June 2006). “CIAO: Chandra’s data analysis system”. In: ed. by David R. Silva and Rodger E. Doxsey. Orlando, Florida , USA, p. 62701V. DOI: 10.1117/12.671760. URL: http://proceedings.spiedigitallibrary.org/proceeding.aspx?doi=10.1117/12.671760 (visited on 09/04/2024).

CXC (Sept. 2024a). *Chandra absolute astrometric accuracy*. URL: https://cxc.harvard.edu/cal/ASPECT/celmon/ (visited on 09/14/2024).

Evans, Ian N. et al. (July 2010). “THE CHANDRA SOURCE CATALOG”. In: *The Astrophysical Journal Supplement Series* 189.1, pp. 37–82. DOI: 10.1088/0067-0049/189/1/37. URL: https://iopscience.iop.org/article/10.1088/0067-0049/189/1/37.

Ginsburg, A. et al. (Mar. 2019). “astroquery: An Astronomical Web-querying Package in Python”. In: *aj* 157. _eprint: 1901.04520, p. 98. DOI: 10.3847/1538-3881/aafc33.

Webb, N.~A. et al. (Sept. 2020). “The XMM-Newton serendipitous survey. IX. The fourth XMM-Newton serendipitous source catalogue”. In: 641, A136–A136. DOI: 10.1051/0004-6361/201937353.

Evans, P.~A. et al. (Jan. 2014). “1SXPS: A Deep Swift X-Ray Telescope Point Source Catalog with Light Curves and Spectra”. In: 210.1, pp. 8–8. DOI: 10.1088/0067-0049/210/1/8.

Evans, P.~A. et al. (Apr. 2020). “2SXPS: An Improved and Expanded Swift X-Ray Telescope Point-source Catalog”. In: 247.2, pp. 54–54. DOI: 10.3847/1538-4365/ab7db9.

Boller, Th. et al. (Apr. 2016). “Second ROSAT all-sky survey (2RXS) source catalogue”. In: 588, A103–A103. DOI: 10.1051/0004-6361/201525648.

Tubín-Arenas, Dusán et al. (Feb. 2024). “The eROSITA upper limits. Description and access to the data”. In: *åp* 682. _eprint: 2401.17305, A35. DOI: 10.1051/0004-6361/202346773.

Kovlakas, K. et al. (Nov. 2020). “A census of ultraluminous X-ray sources in the local Universe”. In: *\mnras* 498.4. _eprint: 2008.10572, pp. 4790–4810. DOI: 10.1093/mnras/staa2481.

Weisskopf, Martin C. et al. (July 2000). “Chandra X-ray Observatory (CXO): overview”. In: *X-Ray Optics, Instruments, and Missions III*. Ed. by Joachim E. Truemper and Bernd Aschenbach. ISSN: 0277-786X. SPIE. DOI: 10.1117/12.391545. URL: http://dx.doi.org/10.1117/12.391545.

Jansen, F. et al. (2001). “XMM-Newton observatory* - I. The spacecraft and operations”. In: *A&A* 365.1, pp. L1–L6. DOI: 10.1051/0004-6361:20000036. URL: https://doi.org/10.1051/0004-6361:20000036.

Gaia Collaboration (Sept. 2016). “The Gaia mission”. In: DOI: 10.1051/0004-6361/201629272. URL: http://arxiv.org/abs/1609.04153.

Gaia Collaboration et al. (July 2022). “Gaia Data Release 3: Summary of the content and survey properties”. In: DOI: 10.1051/0004-6361/202243940. URL: http://arxiv.org/abs/2208.00211.

Helou, G et al. (Jan. 1991). “The NASA/IPAC extragalactic database.” In: ed. by M.~A. Albrecht and D Egret. Vol. 171, pp. 89–106. DOI: 10.1007/978-94-011-3250-3_10.

Wenger, M et al. (Apr. 2000). “The SIMBAD astronomical database. The CDS reference database for astronomical objects”. In: 143, pp. 9–22. DOI: 10.1051/aas:2000332.

Wang, Song et al. (Oct. 2020). “Stellar X-Ray Activity Across the Hertzsprung–Russell Diagram. I. Catalogs”. In: *The Astrophysical Journal* 902.2. Publisher: American Astronomical Society, pp. 114–114. DOI: 10.3847/1538-4357/abb66d.

Lawrence, A et al. (Aug. 2007). “The UKIRT Infrared Deep Sky Survey (UKIDSS)”. In: 379.4, pp. 1599–1617. DOI: 10.1111/j.1365-2966.2007.12040.x.

Ahumada, Romina et al. (July 2020). “The 16th Data Release of the Sloan Digital Sky Surveys: First Release from the APOGEE-2 Southern Survey and Full Release of eBOSS Spectra”. In: 249.1, pp. 3–3. DOI: 10.3847/1538-4365/ab929e.

McMahon, R.~G. et al. (Dec. 2013). “First Scientific Results from the VISTA Hemisphere Survey (VHS)”. In: *The Messenger* 154, pp. 35–37.

Ochsenbein, F., P. Bauer, and J. Marcout (Apr. 2000). “The VizieR database of astronomical catalogues”. In: *åps* 143. _eprint: astro-ph/0002122, pp. 23–32. DOI: 10.1051/aas:2000169.

CXC (Mar. 2024b). *Dictionary: Readout Streak Events - CIAO 4.16*. URL: https://cxc.cfa.harvard.edu/ciao/dictionary/readout_streak.html (visited on 09/14/2024).

Mazzali, Paolo A. et al. (Aug. 2008). “The Metamorphosis of Supernova SN 2008D/XRF 080109: A Link Between Supernovae and GRBs/Hypernovae”. In: *Science* 321.5893. _eprint: 0807.1695, p. 1185. DOI: 10.1126/science.1158088.

Soderberg, A. M. et al. (July 2008). “Erratum: An extremely luminous X-ray outburst at the birth of a supernova”. In: *\nat* 454.7201, p. 246. DOI: 10.1038/nature07134.

Modjaz, M. et al. (Sept. 2009). “From Shock Breakout to Peak and Beyond: Extensive Panchromatic Observations of the Type Ib Supernova 2008D Associated with Swift X-ray Transient 080109”. In: *\apj* 702.1. _eprint: 0805.2201, pp. 226–248. DOI: 10.1088/0004-637X/702/1/226.

Astropy Collaboration et al. (Oct. 2013). “Astropy: A community Python package for astronomy”. In: 558, A33–A33. DOI: 10.1051/0004-6361/201322068.

Astropy Collaboration et al. (Sept. 2018). “The Astropy Project: Building an Open-science Project and Status of the v2.0 Core Package”. In: 156.3, pp. 123–123. DOI: 10.3847/1538-3881/aabc4f.

Astropy Collaboration et al. (Aug. 2022). “The Astropy Project: Sustaining and Growing a Community-oriented Open-source Project and the Latest Major Release (v5.0) of the Core Package”. In: 935.2, pp. 167–167. DOI: 10.3847/1538-4357/ac7c74.